AN AUTOMATED WAVELET ANALYSIS APPROACH TO *TRACE* QUIET SUN OSCILLATIONS

R. T. James M^{c}Ateer[1,*], Peter T. Gallagher[2], David R. Williams[3], D.Shaun Bloomfield[1], Mihalis Mathioudakis[1], and Francis P. Keenan[1]

[*]E-mail: j.mcateer@qub.ac.uk
[1]Department of Pure and Applied Physics, Queen's University Belfast, Belfast, BT7 1NN, N. Ireland, U.K.
[2]L-3 Communications GSI, NASA Goddard Space Flight Center, Greenbelt, Maryland 20771, U.S.A.
[3]Mullard Space Science Laboratory, Holmbury St. Mary, Dorking, Surrey, RH5 6NT, U. K.

ABSTRACT

An automated wavelet analysis approach to *TRACE* UV quiet Sun datasets is discussed. Periodicity and lifetime of oscillations present in the network and internetwork are compared and contrasted. This provides a means of extending previous Fourier results into the time-localised domain. The longest lifetime oscillations occur around the acoustic band and the network tends to dominate over the internetwork at periods > 4 mins. However, it is shown that the internetwork can dominate over the network at long periods (7 – 20 mins), but only for short lifetimes (< 3 complete oscillations). These results are discussed in terms of chromospheric heating theories.

Key words: Sun: oscillations – Sun: chromosphere – Sun: photosphere – Sun: UV radiation – methods: statistical.

1. INTRODUCTION

The subject of chromospheric oscillations and their possible role in chromospheric heating is one of the longest running debates in solar physics. A temperature minimum at $\sim$500 km above the photosphere, and the subsequent reversal of the temperature profile, suggests that some unknown heating mechanism must be present to balance the energy lost by radiation. As this mechanism cannot be due to either conduction or radiation (Narain & Agarwal 1994), chromospheric heating theories have mainly concentrated on heating via the dissipation of energy carried by waves. The oscillatory signaures of these waves as studied in intensity or velocity provides information as to the mode of these waves, whether standing or travelling, and the dominant restoring force (magnetic, gas pressure, gravity, etc.)

The distinct network structure of the quiet Sun provides a spatial dichotomy between the network and internetwork which is also apparent in the Fourier spectrum of lightcurves from these two regions. Wheras the internetwork contains oscillations with periodicities around 180 s

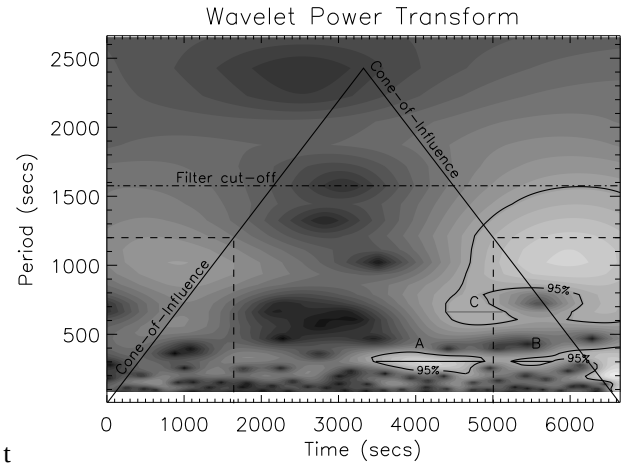

t

Figure 1. Wavelet power transform of a typical network lightcurve. The two slanted lines define the cone-of-influence. The dash-dot line is at 1624 s, the cut-off of the high-pass filter. The contours are at the 95% confidence level. The solid lines at the define the lifetimes of three maxima A, B, and C outside the cone-of-influence

(a broad 3–8 mHz peak in the Fourier spectrum) the network displays longer periodicity (up to 20 mins). This leads to the suggestion that different heating mechanisms may dominate in each region.

Carlsson & Stein (1992, 1997) successfully modelled the well known K_{2v} internetwork grains as upwardly-propagating acoustic waves. Brandt et al. (1992) suggest a scenario whereby there are two types of grains: one with a long term memory, termed 'persistent flashers', with a magnetic dependence; and a second, 5–10 times more common, with no spatial memory or magnetic dependence. Longer-period network oscillations (5–20 mins) have not benefited from similarly detailed simulations, mainly due to the difficulty of modelling the chromospheric plasma in the presence of the kilogauss magnetic fields (Bogdan et al. 2003). Wavelet-based studies (McAteer et al. 2003a) show the existence of mainly upwardly-propagating (but also some downwardly-propagating) waves in the chromosphere at

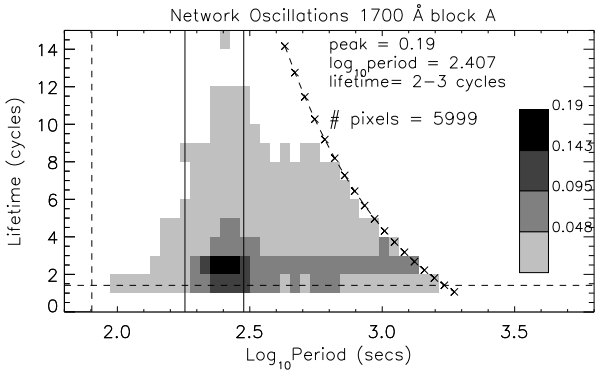

Figure 2. Distribution of periodicity (in $\log_{10}(P)$) and lifetime (in cycles) of oscillations in the network for the first half of the 1700Å dataset. The figure is scaled to the maximum occurrence rate per pixel (0.19). The vertical lines are at 3 and 5 min. The crosses and dashes signify the maximum number of detectable cycles outside the COI at each period.

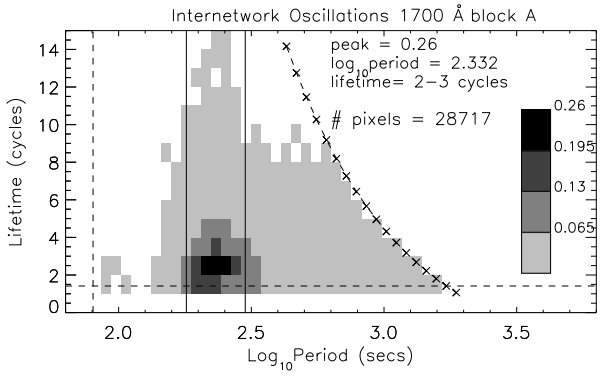

Figure 3. Distribution of periodicity (in $\log_{10}(P)$) and lifetime (in cycles) of oscillations in the internetwork for the first half of the 1700Å dataset. The figure is scaled to the maximum occurrence rate per pixel (0.26). The vertical lines are at 3 and 5 min. The crosses and dashes signify the maximum number of detectable cycles outside the COI at each period.

speeds close to the sound speed. The tendancy of of these oscillations to occur in the very centre of network elements (McAteer et al. 2002), combined with a lack of both intensity and oscillatory power near, but not directly above, photospheric network elements (termed 'magnetic shadows'), suggests the existence of mode-conversion of acoustic waves as they interact with the magnetic canopy (Judge et al. 2001).

The paper extends the previous searches for oscillations by using a automated wavelet-based approach to searching for periodicity in a large number (∼30,000) of lightcurves. The automated approach is essential when dealing with a large number of lightcurves, and is readily applicable to datasets from other regions of the sun and/or other instruments. The wavelet approach, based on one first discussed in Ireland et al. (1999), is preferred over previous Fourier analysis due to the quasi-periodic nature of the oscillations.

2. OBSERVATIONS

A dataset from 1999 May 4 containing quiet-Sun images in the four UV passbands (1700 Å, 1600 Å, 1216 Å, 1550 Å) with a FOV of 128" × 320" was selected for this study. Further details of the dataset can be found in Krijger et al. (2003). A simple investigation into the frame rate stability in each passband resulted in a constant cadence of 40.05 s being assumed. After image 168 there was a 50 s delay, corresponding to a small change in the FOV as *TRACE* compensated for solar rotation. For this reason the data were divided into two equal timeblocks; block A containing images 1–168 and block B containing images 169–336. Any images severely contaminated by cosmic rays were cleaned using programs available in the *TRACE* branch of the SolarSoftWare (SSW; Freeland & Handy 1998) tree of IDL. Network and internetwork masks were created as discussed in McAteer et al (2002, 2003a), and applied to all four UV passbands. This resulted in 5999 network lightcurves and 28717 internetwork lightcurves in each block of each passband.

3. WAVELET ANALYSIS

A wavelet analysis (using a Morlet wavelet, Torrence & Compo 1998) was carried out on every lightcurve. This provides time-localised information as to any periodicity present in each lightcurve. An example wavelet power transform is provided in Fig. 1. Here the abscissa is time, t, and the ordinate is period, P. This is displayed on a linear intensity scale, such that brighter areas correspond to greater oscillatory power. The contours are at the 95% significance level and the two slanted lines define the cone-of-influence (COI). Edge effects are significant above these two lines. As the extent of the COI at each period (dashed lines) is simply the decorrelation time for a spike in the time series, t_d, the maximum possible detectable period is given by

$$\frac{3\sqrt{2}\,\mathrm{P}_{max}}{1.03} = \delta\mathrm{t} \times (\mathrm{N}-1), \qquad (1)$$

where δt is the cadence, and N is the number of data points in the lightcurve (hence $\delta\mathrm{t} \times (\mathrm{N}-1)$ is the total duration of the lightcurve). Rearranging,

$$\mathrm{P}_{max} = \frac{1.03 \times 40.05 \times 167}{3\sqrt{2}} = 1642\ \mathrm{s}, \qquad (2)$$

which is the dash-dot line on Fig. 1 and was used as the cut-off for the high pass filter carried out on each lightcurve (McAteer et al. 2003b).

For each filtered lightcurve, an automated routine searched for both periodicity and lifetime of any oscillatory power maxima (Fig. 1). The lifetime, l, is defined as

$$l = \frac{t_{end} - t_{start}}{P}, \qquad (3)$$

where t_{start} is the time when the power intially goes above 95% significance, and t_{end} the time when the

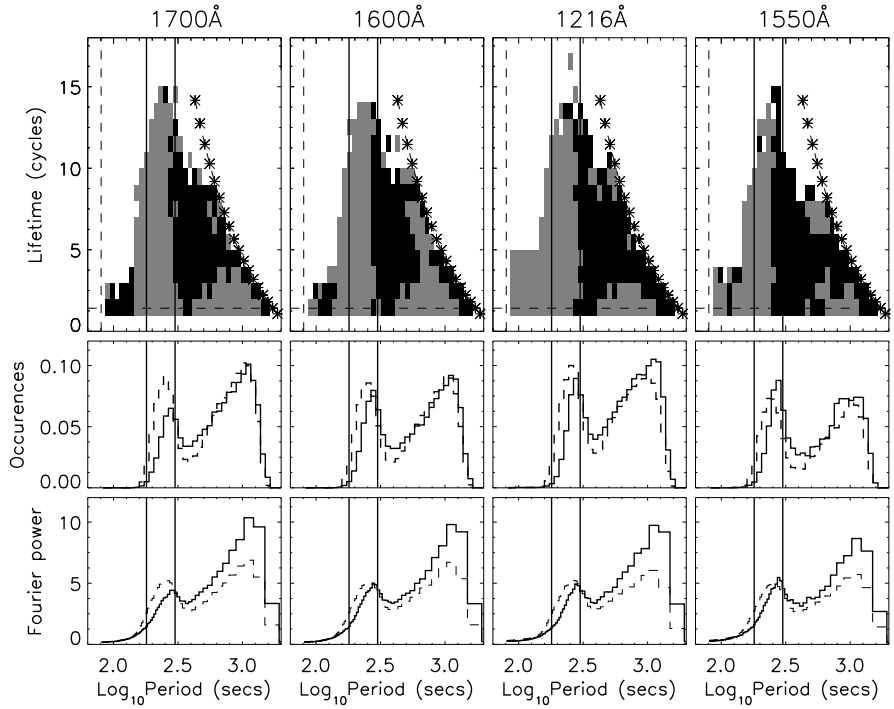

Figure 4. Columns: Increasing height of formation from left to right; 1700 Å, 1600 Å, 1216 Å, 1550 Å. Rows: Top - Same axis and lines as Fig. 2 and Fig. 3. Grey areas are where the internetwork displays more oscillations, black areas are where the network display more oscillations, for each period and lifetime. Middle - Occurrence rate per pixel averaged over all lifetimes for the network (solid) and internetwork (dashed). Bottom - Average Fourier power per pixel at each period for network (solid) and internetwork (dashed).

power dips below 95% significance. This provides an lifetime estimate in terms of total number of oscillations.

4. RESULTS

Typical results from all network and internetwork lightcurves are presented in Fig. 2 and Fig. 3 respectively for the first half of the 1700Å dataset. Here the ordinate is the period, P, as determined from the wavelet analysis. The nature of wavelet analysis means that the values of period increase logarithmically. The abscissa, l, is the oscillation lifetime binned to integer values. The horizontal dashed line is at $\sqrt{2}/1.03$ cycles (minimum lifetime), the vertical dashed line is at the Nyquist frequency, while the two solid vertical lines are at 3 and 5 min. The curved dashed line refers to the maximum number of complete cycles which can be observed at each period (due to the finite length of the time series). Both figures are plotted on a inverted linear intensity scale, such that darker areas correspond to a larger number of pixels with oscillations at period P, for lifetime l. The four colour bands refer to the upper quartile (black; $> 75\%$ of peak value), mid-upper quartile (dark grey; 50–75% of peak value), mid-lower quartile (light grey; 25–50% of peak value) and lower quartile (lightest grey; $< 25\%$ of peak value). The data have been divided by the number of pixels (hence number of lightcurves), to make all results from the network and internetwork directly comparable.

A comparison of network and internetwork oscillations is presented in Fig. 3. In each bandpass, an average network and internetwork lifetime-period diagram was created. The comparison diagram was then created by comparing the network occurrence rates to the internetwork occurrence rates at each period and lifetime. In each column, the top part has the same axes and lines as Fig. 2 and Fig. 3. Black parts of the top row of Figure 3 refer to where the network has a greater occurrence rate, whereas grey parts refer to where the internetwork dominates. The middle and bottom row of Figure 3 display the average Fourier power and occurence rate per pixel. In these plots, the solid line refers to network data, and a dashed line to internetwork.

5. DISCUSSION

5.1. Long Lifetime Oscillations

During each cycle, a wave may transfer a portion of its energy to the surroundings. Hence, any long-lifetime oscillations (LLOs), which undergo several complete cycles, are good candidates for chromospheric heating. In all the UV passbands, in both the network and internetwork, all the LLOs occur near the acoustic band. At longer periods, oscillations tend to last for fewer cycles, and are even more transient at shorter periods. As these oscillations do not seem to recur it is believed that the

source, in driving the LLO, no longer has sufficient energy to create further oscillations.

5.2. Peak Periodicity Comparison

As often confirmed before, the network tends to oscillate with a peak period close to 5 min. The internetwork, whilst exhibiting many more oscillations around 3 min, contains a peak close to 4 min. The 50% reccurrence rate of oscillations near the peak in each case suggest some degree of spatial memory. The network contains an extended tail at the 25–50% level up to periods of $\log_{10}(P)$=2.9 ($P\sim$800 s). Hasan & Kalkofen (1999) suggest a scenario whereby kink-mode waves generated in the photospheric network may travel up through the chromosphere, before coupling with saugage-mode waves. The extended tail of the network oscillations in Figure 2 may be the oscillatory signature of the kink-mode wave at P=534 s ($\log_{10}(P)$=2.73)

5.3. Network - Internetwork Comparison

It is clear from the middle and bottom rows of Fig. 3 that the network has greater oscillatory power at all periods longer than $\log_{10}(P)$=2.45 ($P\sim$280 s; 3.6 mHz). There is also a tendency for this cross-over period to decrease with increasing HOF (from $\sim$300 s in 1700 Å to $\sim$250 s in 1550 Å). However the top row in Figure 3 displays a further feature. If the network dominates for all lifetimes at periods above $\log_{10}(P)$=2.45, then the resulting plots in the top row should be entirely black to the right of this cross-over, and entirely grey to the left of this cross-over. Instead there are regions of internetwork domination above $\log_{10}(P)$=2.45 for a small number of cycles. This mixing is more prevalent in the 1700 Å and 1600 Å data than for the 1216 Å and 1550 Å, suggesting these short-lifetime, long-period internetwork oscillations are most likely a low-chromosphere phenomenon. There is also some mixing at short periods, which may be examined further by using a higher-cadence dataset.

5.4. Future work

A study into the spatial position of pixels displaying different periodicities and lifetimes may answer some of the questions posed in this paper. It may be useful to apply this method to higher-cadence *TRACE* quiet-Sun datasets and other instruments. In a wider context, this technique can be used in other areas of solar physics (e.g., active regions) or astronomy in general where a search for transient, spatially-localised, oscillatory power is required (e.g., multi-target wide-field imaging).

REFERENCES

Bogdan, T. J., et al. 2003, ApJ, submitted

Brandt, P. N., Rutten, R. J., Shine, R. A., & Trujillo Bueno, T. 1992, in Cool Stars, Stellar Systems, and the Sun, Proc. 7th Cambridge Workshop, eds M. S. Gaimpapa & J. A. Bookbinder, 26, 121

Carlsson, M., & Stein, R. F. 1992, ApJ, 397, L59

Carlsson, M., & Stein, R. F. 1997, ApJ, 481, 500

Freeland, S. L., & Handy, B. N. 1998, Sol. Phys., 182, 497

Hasan, S. S., & Kalkofen, W. 1999, ApJ, 512, 899

Ireland, J., Walsh, R. W., Harrison, R. A., & Priest, E. R. 1999, A&A, 347, 355

Judge, P. G., Tarbell, T. D., & Wilhelm, K. 2001, ApJ, 554, 424

Krijger, J. M., Heinzel, P., Curdt, W., & Schmidt, W. 2003, A&A, sub

McAteer, R. T. J., Gallagher, P. T., Williams, D. R., Mathioudakis, M., Phillips, K. J. H., & Keenan, F. P. 2002, ApJ, 567, L165

McAteer, R. T. J., Gallagher, P. T., Williams, D. R., Mathioudakis, M., Bloomfield, D. S., Phillips, K. J. H., & Keenan, F. P. 2003a, ApJ, 587, 806

McAteer, R. T. J., Gallagher, P. T., Bloomfield, D. S., Williams, D. R., Mathioudakis, M., & Keenan, F. P. 2003b, ApJ, in press

Narain, U., & Agarwal, P. 1994, Bull. Astr. Soc. India, 22, 111

Torrence, C. & Compo, G. P. 1998, Bull. Amer. Meteor. Soc., 79, 61